Electronic Supplementary Material (ESI) for Journal of Materials Chemistry C.

Supporting Information

Boosting the photocatalytic activity of graphite carbon nitride by design of novel MoS_2-transition metals heterojunctions cocatalyst

Kui Li,* Ye-Zhan Lin, Yu Zhang, Mei-Ling Xu, Ling-Wang Liu and Fu-Tian Liu

School of Materials Science and Engineering, University of Jinan, Jinan 250022, China

Email: mse_lik@ujn.edu.cn.

Characterization Methods

The powder X-ray diffraction (XRD) patterns were recorded on a D/max 2500 VL/PC diffractometer (Japan) equipped with graphite monochromatized Cu Kα radiation (λ = 1.54060 Å), and the corresponding work voltage and current was 40 kV and 100 mA, respectively. The transmission electron microscopy (TEM) and high-resolution TEM (HRTEM) images were recorded on JEOL-2100F apparatus at an accelerating voltage of 200 kV. Surface morphologies of the g-C_3N_4-based heterostructures were examined by a scanning electron microscope (SEM, JSM-7600F) at an acceleration voltage of 10 kV, and the elemental mapping was performed with JSM-5160LV-Vantage typed energy dispersive X-ray spectroscopy (EDS) spectrometer. Element content analysis was tested on an inductively coupled plasma (ICP) spectroscope (Agilent ICP0ES730, America). The UV−Vis absorption and diffused reflectance spectra were recorded using a Cary 5000 UV-Vis spectrometer (Viarian, USA) with $BaSO_4$ as a reflectance standard. Steady photoluminescence (PL) emission spectra were tested by a luminescmce spectrophotometer (QM-400, PTI) with 350 nm excitation wavelength.

Electrochemical measurements

All the electrochemical experiments were conducted on the electrochemical station (Bio-Logic SP-150) in a three-electrode system at room temperature with a glassy carbon electrode (3 mm in diameter), (sheet resistance 20−25 Ω/square) as the working electrode, a platinum wire as the auxiliary electrode, and an Ag/AgCl electrode as the reference electrode. For the electrochemical measurements, 4 mg of the catalysts were dispersed in 2 mL of 9:1 v/v water/Nafion by sonication to form a homogeneous ink. Typically, 5 μL well-dispersed catalysts were covered on the glassy carbon electrode and then dried in an ambient environment for measurements. The electrocatalyst was prepared with a catalyst loading of 0.14 mg cm^{-2}. The electrolyte of transient photocurrent responses experiments, electrochemical impedance spectroscopy (EIS), and Mott-Schottky (M-S) was 0.5 M Na_2SO_4 aqueous solution, and the electrolyte of linear sweep voltammetry (LSV) was in 1M KOH solutions for the HER and OER results. EIS was performed at an impressed voltage of -0.3 eV, for voltage ranging from -2.5 V to 2.5 V. M-S was measured for a scan voltage ranging from -1 V to 0.5 V at 500-2000 Hz. The transient photocurrent responses measurement was performed under full light irradiation, and the LSV obtained at a scan rate of 1 mV/s.

Photocatalytic hydrogen evolution

The photocatalytic H_2-production experiments were performed via a photocatalytic H_2-production activity evaluation system (CEL-SPH2N, CEAULight, China) in a 300 mL Pyrex flask, and the openings of the flask were sealed with silicone rubber septum. A 300 W xenon arc lamp, which was positioned 13 cm away from the reaction solution, was used as an all light source to trigger the photocatalytic reaction. A 300 W xenon arc lamp with and without a UV-cutoff filter with a wavelength range of 420 ~ 800 nm, which was positioned 13 cm away from the reaction solution, was used as a visible light source to trigger the photocatalytic reaction. The focused intensity on the flask was ~ 200 $mW \cdot cm^{-2}$, which was measured by a FZ-A visible-light radiometer (made in the photoelectric instrument factory of Beijing Normal University, China). In a typical photocatalytic H_2-production experiment, 50 mg of the as-prepared photocatalyst was suspended in 50 mL of mixed aqueous solution containing 5 ml $C_6H_{15}NO_3$ (TEOA, AR,98%). Before irradiation, the system was vacuumed for 5 min via the vacuum pump to completely remove the dissolved oxygen and ensure the reactor was in an anaerobic condition. A continuous magnetic stirrer was applied at the bottom of the reactor to keep the photocatalyst particles in suspension during the experiments. H_2 content was analyzed by gas chromatography (GC-7900, CEAULight, China). All glasswares were carefully rinsed with DI water prior to usage. The photocatalytic stability was performed in the same processing parameters.

Supporting Figures

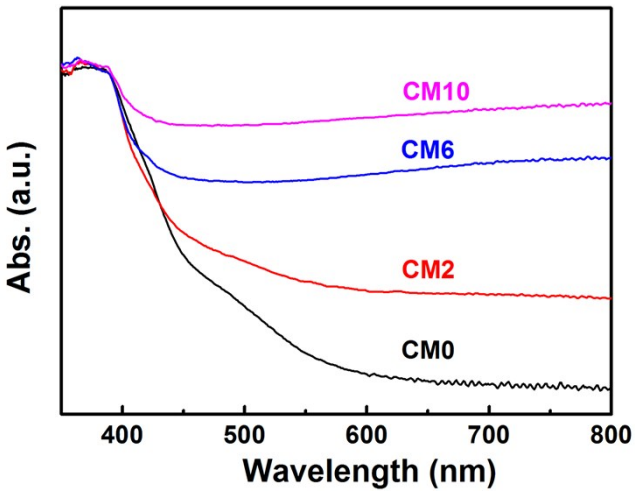

Fig. S1. Effect of amount of MoS_2 on the UV−visible diffuse reflection spectra in g-C_3N_4-MoS_2 heterostructures.

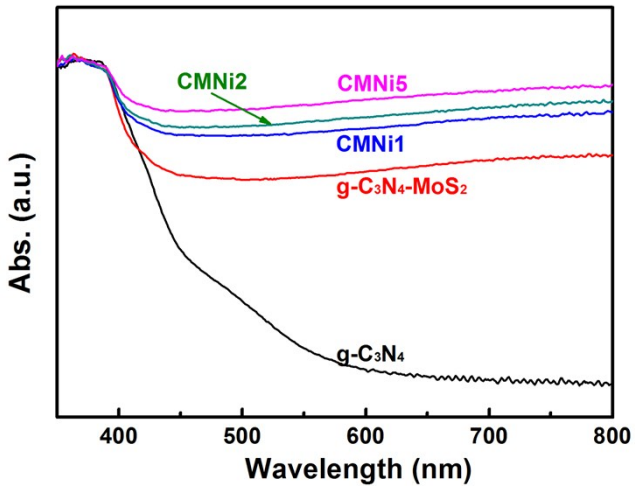

Fig. S2. Effect of amount of Ni on the UV−visible diffuse reflection spectra in g-C_3N_4-MoS_2-Ni ternary heterostructures.

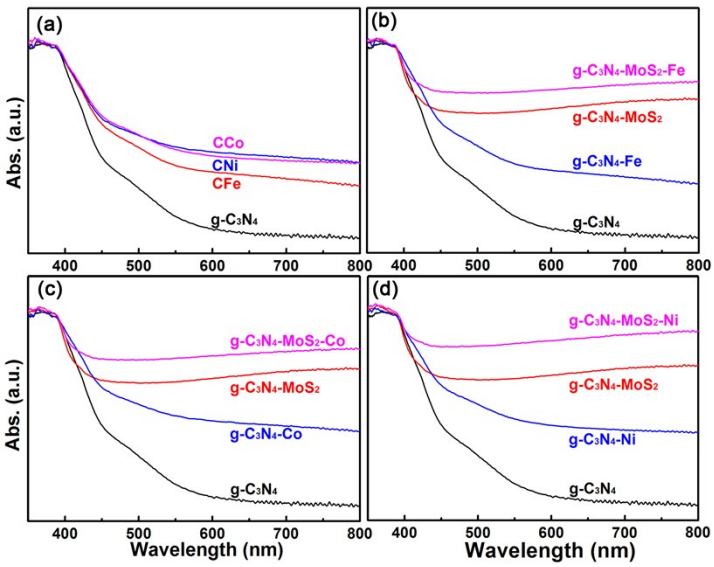

Fig. S3. (a) Effect of types of metal on the UV−visible diffuse reflection spectra in g-C_3N_4-metal heterostructures. The comparison results of the UV−visible diffuse reflection spectra of g-C_3N_4, g-C_3N_4-metals, g-C_3N_4-MoS_2, and g-C_3N_4-MoS_2-metals, with metals of (b) Ni, (c) Co and (d) Fe.

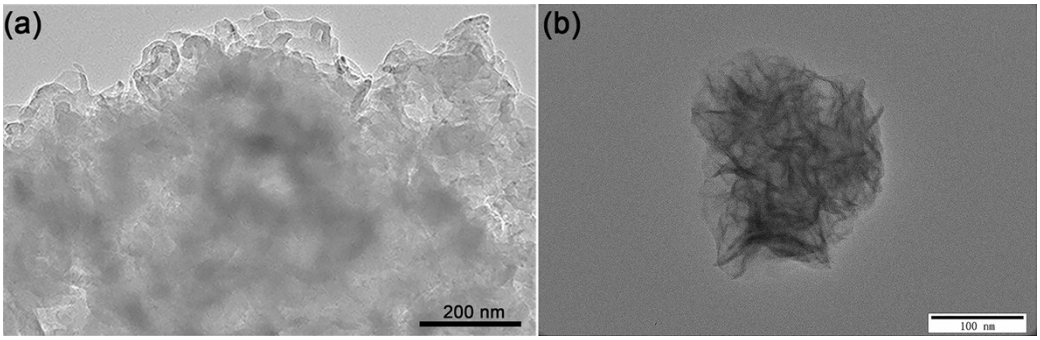

Fig. S4. Transmission electron microscopy (TEM) images of the (a) pristine g-C_3N_4 and (b) MoS_2 derived from PMo_{12}.

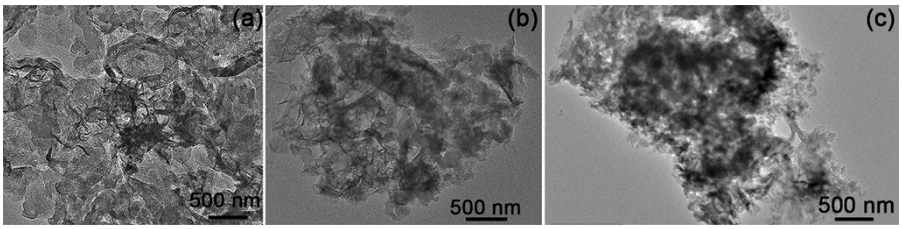

Fig. S5. The TEM images of (a) g-C_3N_4-MoS_2-Fe, (b) g-C_3N_4-MoS_2-Co and (c) g-C_3N_4-MoS_2-Ni.

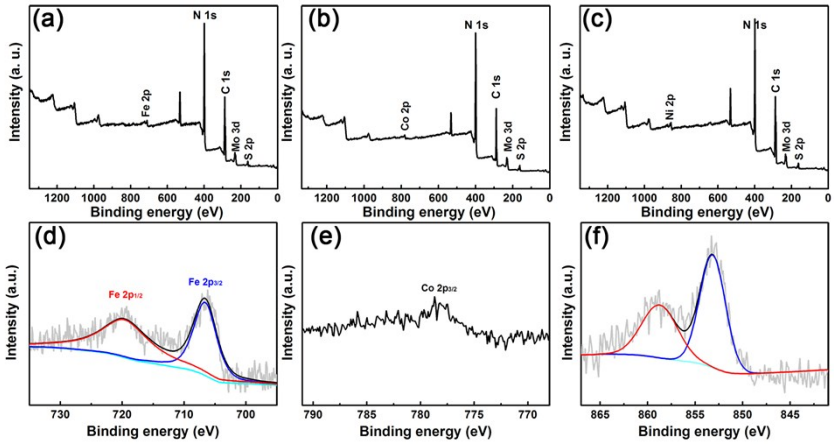

Fig. S6. The survey XPS spectrum of (a) g-C_3N_4-MoS_2-Fe, (b) g-C_3N_4-MoS_2-Co and (c) g-C_3N_4-MoS_2-Ni ternary heterostructures, and high-resolution XPS spectra of (d) Fe 2p, (e) Co 2p and (f) Ni 2p in g-C_3N_4-MoS_2-Fe, g-C_3N_4-MoS_2-Co and g-C_3N_4-MoS_2-Ni, respectively.

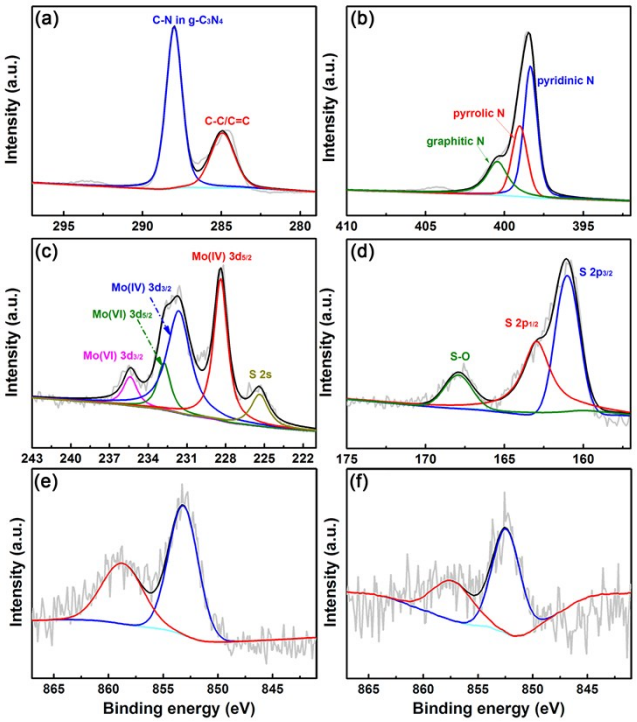

Fig. S7. The high-resolution XPS spectra of (a) C 1s, (b) N 1s, (c) Mo 3d and (d) S 2p in g-C_3N_4-MoS_2-Ni after the photocatalytic stability test, and Ni 2p in g-C_3N_4-MoS_2-Ni (e) before and (f) after the photocatalytic stability measurement. In comparison with the corresponding elemental spectrum in pristine g-C_3N_4-MoS_2-Ni in Fig. 4c, the binding energy of the deconvoluted peaks didn't change, verifying its good photocatalytic stability.

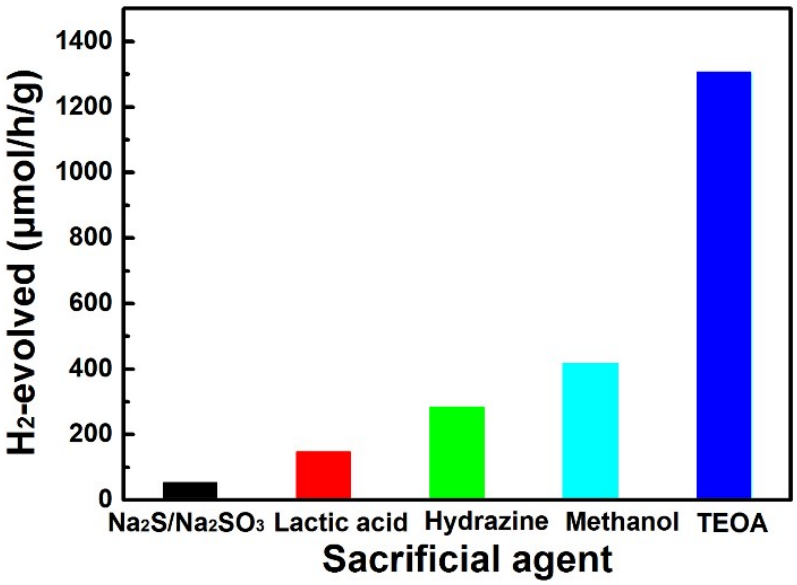

Fig. S8. Effect of the types of sacrificial agents (Na_2S (0.35 M)/Na_2SO_3 (0.25 M) mixed solution, lactic acid (10 vol%), hydrazine (10 vol%), methanol (10 vol%) and TEOA (10 vol%)) on the photocatalytic hydrogen production activity of g-C_3N_4-MoS_2-Ni under visible light irradiation.

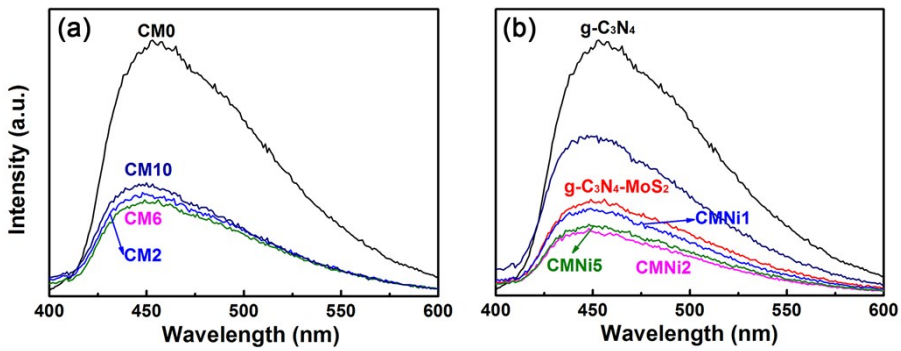

Fig. S9. The PL spectra of the g-C_3N_4-based samples with different amounts of (a) MoS_2, and (b) Ni.

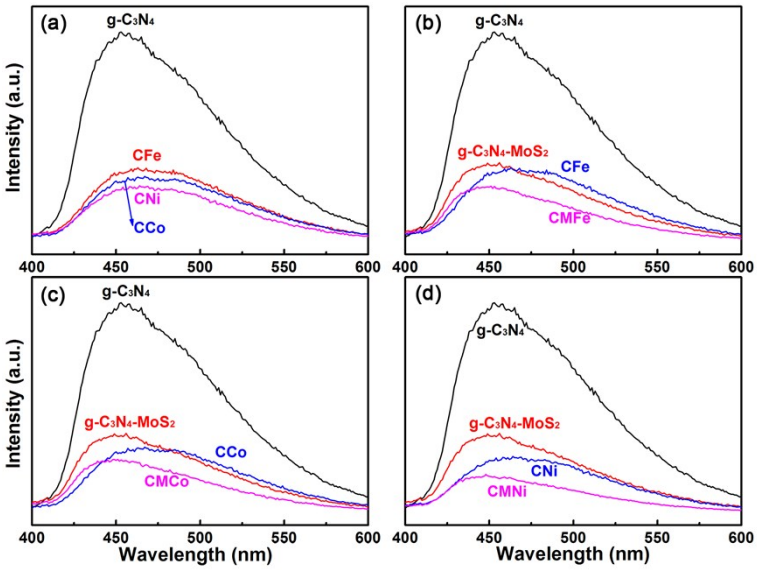

Fig. S10. (a) Effect of types of metal on the PL spectra in g-C_3N_4-metal heterostructures. The comparison results of the PL spectra of g-C_3N_4, g-C_3N_4-metals, g-C_3N_4-MoS_2, and g-C_3N_4-MoS_2-metals, with metals of (b) Fe, (c) Co and (d) Ni.

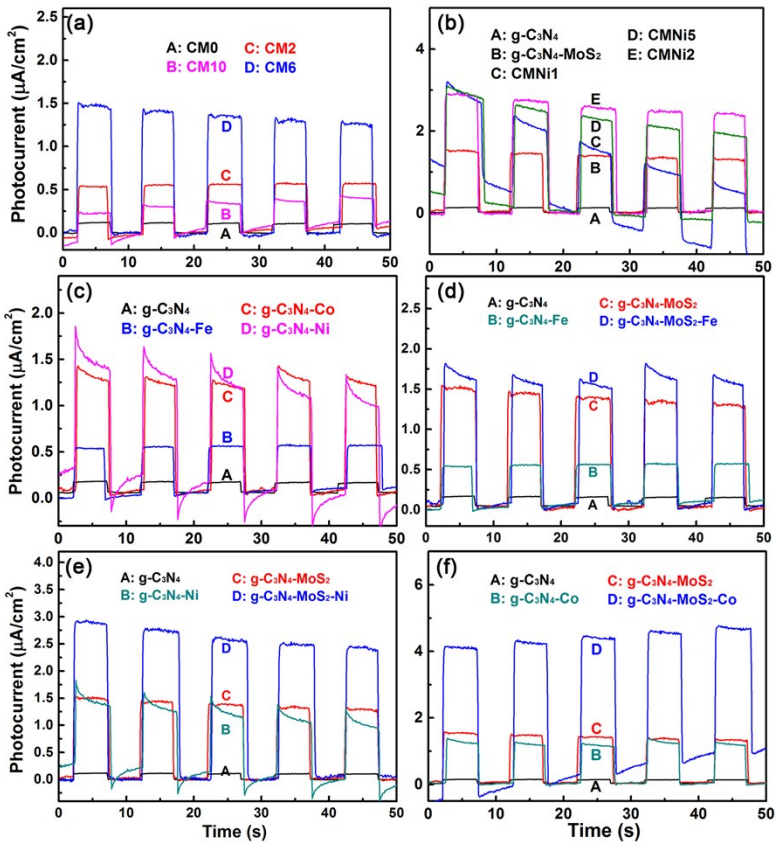

Fig. S11. Effect of amount of (a) MoS_2 and (b) Ni on the transient photocurrent responses in g-C_3N_4-based heterostructures. (c) Effect of types of metal on the transient photocurrent responses in g-C_3N_4-metal heterostructures. The comparison results of the transient photocurrent responses of g-C_3N_4, g-C_3N_4-metals, g-C_3N_4-MoS_2, and g-C_3N_4-MoS_2-metals, with metals of (d) Fe, (e) Ni and (f) Co.

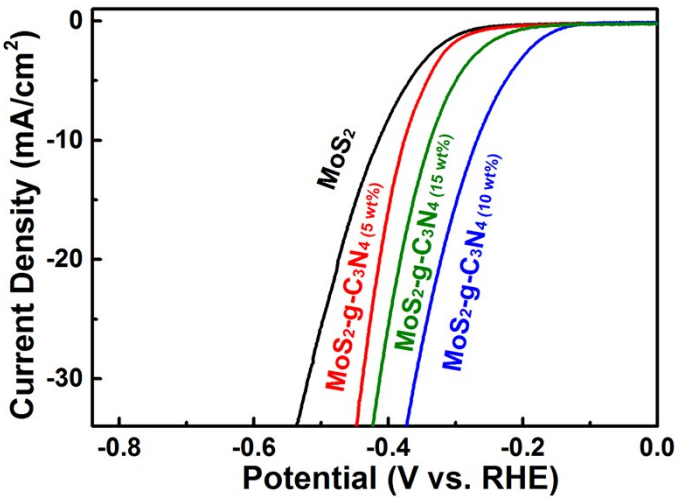

Fig. S12. Effect of amount of g-C_3N_4 on the electrocatalytic HER performance of MoS_2-g-C_3N_4 heterostructures. Adoption of small amount of g-C_3N_4 could dramatically improve the electrocatalytic HER performance of MoS_2, which was consistent with that the modified g-C_3N_4 could also exhibit the excellent electrocatalytic activity reported in previous publication (*J. Am. Chem. Soc.* 2017, **139**, 3336−3339 and *Adv. Funct. Mater.* **2017**, 1606352), and the MoS_2-g-C_3N_4 with 10 wt% g-C_3N_4 (weight ratio of MoS_2/g-C_3N_4 was nearly 10) exhibited the optimal electrocatalytic HER activity.

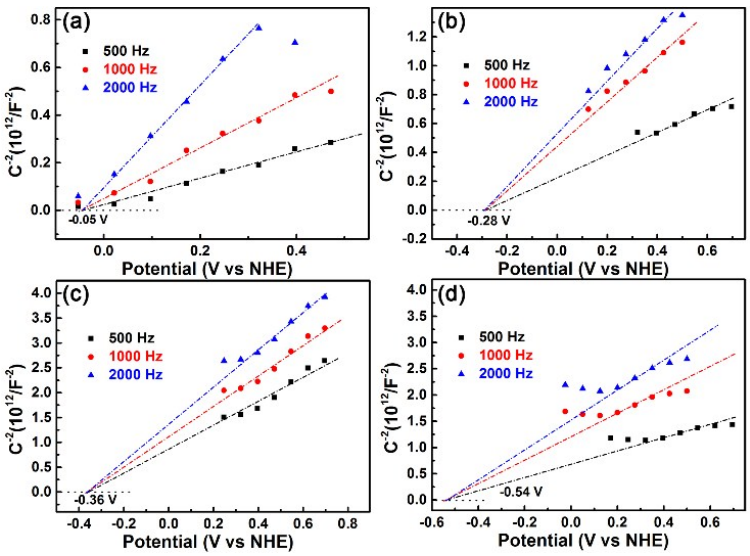

Fig. S13. The Mott−Schottky plots of (a) MoS_2, (b) MoS_2-Fe, (c) MoS_2-Co and (d) MoS_2-Ni.

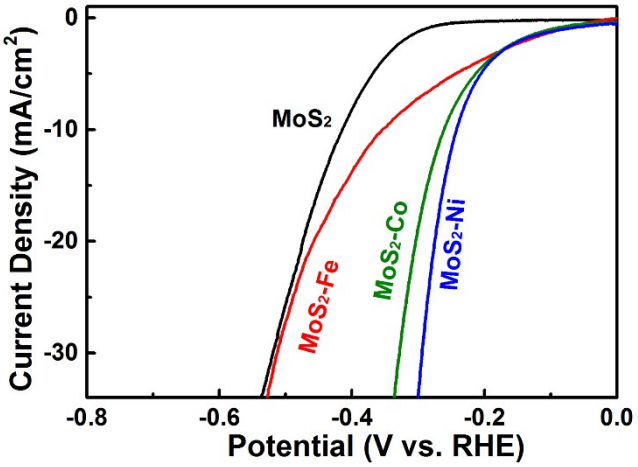

Fig. S14. Effect of types of metals on the electrocatalytic HER performance of MoS_2. The adoption of Ni could dramatically raise the electrocatalytic HER performance as confirmed by the lower HER overpotential and larger current density. This result indicated the MoS_2-metal heterojunction could acted as more effective cocatalyst for improving the photocatalytic activity of g-C_3N_4 as verified by its better HER performance.